Reaction Kinetics Study of Short DNA Strands Using a Maximum Entropy Method and Nonlinear Curve Fitting

Taegon Kim,[†] Ja Eun Lee,[†] Sangwook Lee,[†] Soo Yong Kim,[†] and Sok Won Kim*[,‡]

Department of Physics, Korea Advanced Institute of Science and Technology, Daejeon 305-701, Korea, and Department of Physics, University of Ulsan, Ulsan 680-749, Korea

Received: July 07, 2008; Revised Manuscript Received: September 02, 2008

It is important to understand the formation of double-strand DNA (dsDNA) in a salt solution because it is one of the key reactions in life. A short cDNA strand pair was designed, and each single-strand DNA (ssDNA) was attached to a fluorescent dye that was either a donor or an acceptor of fluorescence resonance energy transfer. The fluorescence intensity was expected to change as time passed as the complementary pairs of ssDNAs formed dsDNAs. The concentration of dsDNA was theoretically calculated, and the measured data were consistent with theoretical results. The analysis of the nonlinear fitting method and the maximum entropy method detected that the reaction curve contains two major types of kinetics that likely represent the formation of dsDNA and mismatching.

1. Introduction

The DNA strand as a biophysical sample has been widely used because it is easy to work with and is important in biology. A complementary pair of single-strand DNA (ssDNA) forms double-strand DNA (dsDNA) with the conformation of double helix under the proper circumstances. It is usually possible to quantify the amount of matched and mismatched pairs in the solution by measuring the UV absorbance. However, this method, while capable of detecting the static fraction, cannot detect dynamic decomposition and composition processes.

Recently, fluorescence spectroscopy has been utilized to investigate dynamic regimes. Reaction dynamics can assist with the understanding of the conformational change of samples. For example, the conformational change of DNA or of a protein can be determined by the diffusion single particle fluorescence resonance energy transfer (spFRET),[1,2] fluorescence correlation spectroscopy (FCS),[3] or fluorescence cross-correlation spectroscopy (FCCS).[4] Despite the advantages of using the aforementioned techniques, they require bulky optics and their validity can be proved only in extremely dilute solutions.

In this article, experimental results from time-varying FRET measurements[5−7] of a dense solution are presented. These results are analyzed with a nonlinear fitting method as well as a maximum entropy method.[11−14] This analysis allows easy access to the kinetics without the need for expensive devices or a large number of parameters. It is expected that the kinetics in the solution will offer clues regarding the structures of transiently formed variants.

2. Experimental Section

Two ssDNA strands were formulated as a complementary pair. The first was 5′ modified with Cy5 5′-TCC TTA CGT-3′, and the second was 5′ modified with Cy3 5′-ACG TAA GGA-3′. The former is termed here as 5′-Cy5-ST-1 and the latter as 5′-Cy3-ST-2. NaCl solution (200 mM) was used as the buffer solution in this work. Figure 1 shows the theoretically predicted temperature-dependent concentration change in the presence of 200 mM NaCl for this pair.[8] The temperature was held at 23 °C during the experiment. This is below the melting temperature.[8,9]

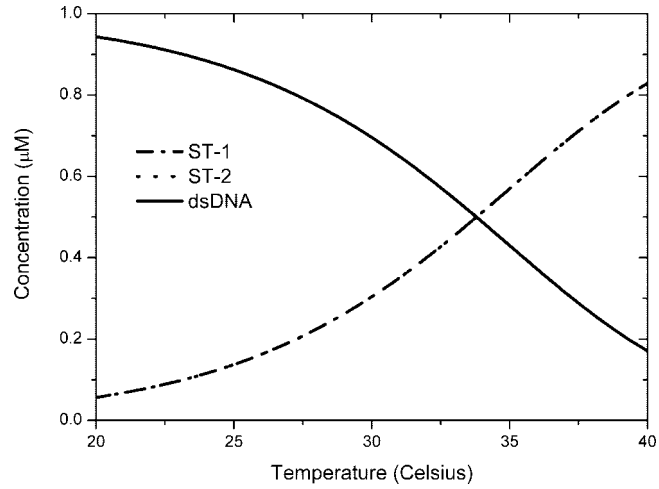

Figure 1. Temperature-dependent concentration of dsDNA (solid line), ST-1 (strand-1, dashed-dotted line), and ST-2 (strand-2, dotted line). The curves of ST-1 and ST-2 overlay each other.

All of the fluorescence signals were measured by spectrofluorometer (model SLM-8100). The excitation beam was generated by a typical xenon arc lamp. The experimental samples were put into a standard quartz cuvette able to transmit 200−2500 nm of light. The concentration of 5′-Cy3-ST-2 was fixed at 1 μM, and the 5′-Cy5-ST-1 was varied at concentrations of 0.2, 0.4, 0.6, 0.8, and 1.0 μM. An injection of 5′-Cy5-ST-1 was initiated near the upper surface of the prefilled 5′-Cy3-ST-2. Time series data acquired during an injection were calibrated and discarded when the entire set of kinetic data was analyzed.

For the kinetics curve, the filter of the excitation beam was set to 549 nm, at which point Cy3 would be excited maximally. The filter of the emission beam was set to 659 nm, where Cy5 would give the maximum emission. To ensure viable detection of the reaction kinetics, several time resolutions were tested. Finally, the spectrofluorometer integrated the signal for 9.4 ms, and 10 ms of time resolution was taken.

* To whom correspondence should be addressed. E-mail: sokkim@ulsan.ac.kr.
† Korea Advanced Institute of Science and Technology.
‡ University of Ulsan.

10.1021/jp8059695 CCC: $40.75
Published on Web 11/06/2008

In the case of the emission scan, the filter of the excitation beam was set as in the aforementioned test, and the fluorescence intensity was measured at steps of 1 nm in the range of 450−750 nm. The measurement and processing time was 0.5 s at steps of 1 nm.

3. Analysis

Calculations of the FRET efficiency were made to verify that the experimental conditions were consistent. From Förster's theory,[5−7] the FRET efficiency of a donor and acceptor pair is given by

$$E_{\text{pair}} = \frac{{R_0}^6}{{R_0}^6 + r^6} \tag{1}$$

Here, r corresponds to the real distance between the donor and acceptor. R_0 denotes the Förster distance, which is given by

$$R_0 = \left(\frac{9000(\log 10) k^2 Q_{\text{D}}}{128 \pi^5 n^4 N_{\text{A}}} \int_0^\infty F_{\text{D}}(\lambda) \varepsilon_{\text{A}}(\lambda) \lambda^4 \, \text{d}\lambda \right)^{\frac{1}{6}} \tag{2}$$

In these experiments, it is necessary to consider the strands that did not form dsDNAs (Figure 1).[10] Assuming that every fluorophore scatters the incident beam, that donor is "off" according to the FRET efficiency when FRET occurs; this, coupled with the assumption that the acceptor gives a slight signal at the wavelength of donor emission maximum, allows the following equation to be deduced:

$$\frac{C_{\text{pair}}}{C_{\text{pair}} + C_{\text{donor}}} E_{\text{pair}} \geq 1 - \frac{2I_{\text{DA}}}{I_{\text{D}}} \tag{3}$$

I_{D} denotes the donor intensity before the injection, and I_{DA} is the donor intensity after the injection. C_{pair} and C_{donor} represent the concentration of dsDNA and ssDNA (donor included) in the final solution. The factor 2 on the right side is unique to this experiment, as the total volume is doubled after the injection. The right side consists of the variables from the measurement, and the left side consists of the theoretically predicted variables. In eq 3, inequality is introduced, as there are several possible causes that may underestimate the extent of FRET phenomena: changes of the optical density of the solution along concentration,[7] overestimation of κ^2,[12−15] and "cross talk" between donor and acceptor.[10,11]

To analyze the reaction kinetics for dsDNA and ssDNA, both the maximum entropy method (MEM) and nonlinear curve fittings were used. The time series of rising kinetics from the experiment did not fit a simple exponential function very well. Thus, there were likely mainly two time scales: a fast scale and a slow scale. Even if the data resulted from several dynamics with different reactions, the result was feasible as a two-exponential fit could reflect it as the mean. Nonlinear least-squares fitting of the data was performed using the following equation:

$$I(t) = I_0 + A_1[1 - \exp(-t/\tau_1)] + A_2[1 - \exp(-t/\tau_2)] \tag{4}$$

where $I(t)$ is the intensity at time t, and I_0 is the intensity at $t = 0$.

The MEM was also used to fit the reaction curves. MEM is widely used to reconstruct images from noisy and incomplete information. It was originally used to enhance astrophysical images,[16] and recently biochemical applications involving this method have emerged.[17−19]

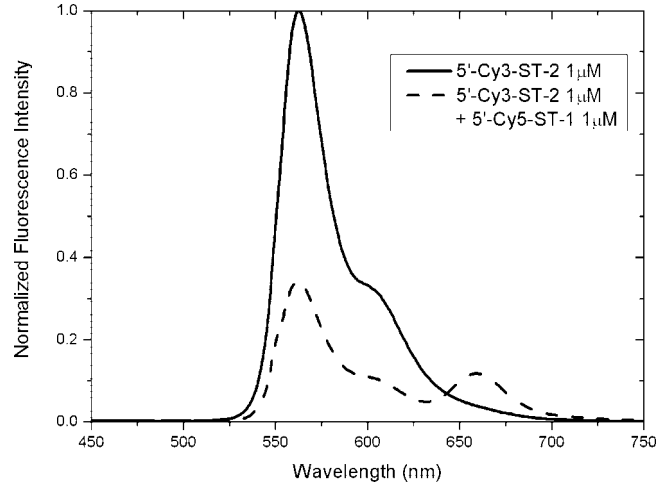

Figure 2. Emission scan of 5′-Cy3-ST-2 1.0 μM by itself (solid line), and the 5′-Cy5-ST-1 1.0 μM and 5′-Cy3-ST-2 1.0 μM mixed solution (dashed line).

MEM fits the intensity data as time passes using the following equation:

$$I(t_i) = -D_0 \int_{-\infty}^{\infty} \text{d} \log \tau [p(\log \tau) \exp(-t_i/\tau)] + \text{baseline} \tag{5}$$

where p is the distribution of $\log \tau$. To optimize such a fitting, MEM sets "entropy" S by

$$S = -\sum_i p_i \log p_i \tag{6}$$

and then maximizes Q by

$$Q \equiv S - \lambda \chi^2 \tag{7}$$

where

$$\chi^2 = \frac{1}{N} \sum_{i=1}^{N} \left(\frac{I_i - I_i^{\text{fit}}}{\sigma_i} \right)^2 \tag{8}$$

At this point, it is possible to calculate the residues:

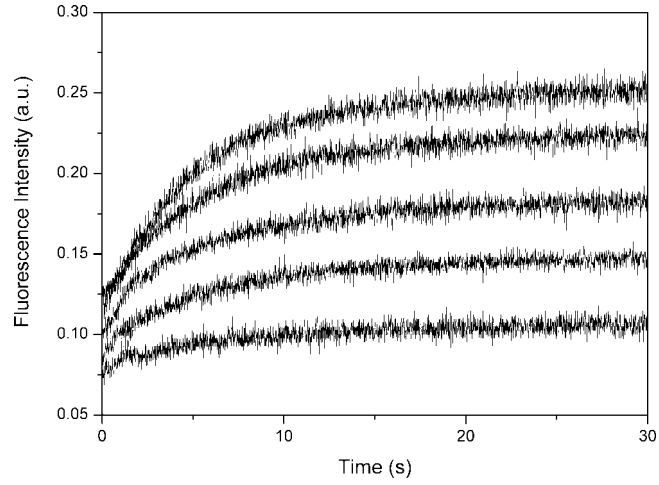

Figure 3. Fluorescence intensity curve as time passes. From the upper curve, each curve represents a mixed solution of 5′-Cy3-ST-2 1.0 μM and 5′-Cy5-ST-1 1.0 μM, 5′-Cy3-ST-2 1.0 μM and 5′-Cy5-ST-1 0.8 μM, 5′-Cy3-ST-2 1.0 μM and 5′-Cy5-ST-1 0.6 μM, 5′-Cy3-ST-2 1.0 μM and 5′-Cy5-ST-1 0.4 μM, and 5′-Cy3-ST-2 1.0 μM and 5′-Cy5-ST-1 0.2 μM.

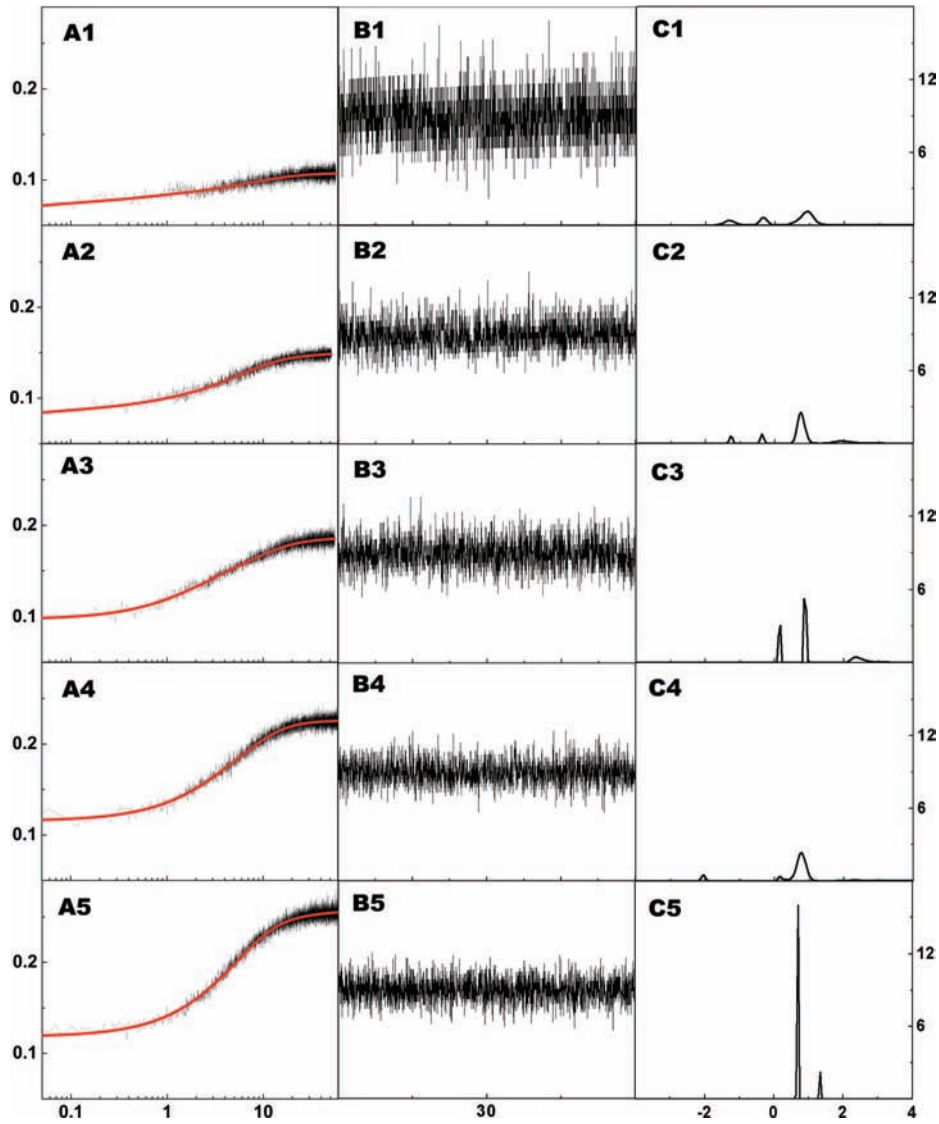

Figure 4. MEM fit results. (A1−A5) MEM fit (red, solid, and smooth line) and real data in log scale (black, solid, and noisy line). (B1−B5) Residue of each fit. (C1−C5) Distribution of log τ. Each row corresponds to each concentration condition. 1: 5′-Cy3-ST-2 1.0 μM and 5′-Cy5-ST-1 0.2 μM, 2: 5′-Cy3-ST-2 1.0 μM and 5′-Cy5-ST-1 0.4 μM, 3: 5′-Cy3-ST-2 1.0 μM and 5′-Cy5-ST-1 0.6 μM, 4: 5′-Cy3-ST-2 1.0 μM and 5′-Cy5-ST-1 0.8 μM, 5: 5′-Cy3-ST-2 1.0 μM and 5′-Cy5-ST-1 1.0 μM.

$$R_i = (I_i - I_i^{\text{fit}})/\sigma_i \tag{9}$$

Steinbach's algorithm[19] was then adopted and the parameters used with it were optimized.

4. Results

Figure 2 shows the emission scan of the fluorescence signal of the solution of 5′-Cy3-ST-2 by itself (solid line) and 5′-Cy3-ST-2 mixed with 5′-Cy5-ST-1 (dashed line) as a simple calibration. The existence of 5′-Cy5-ST-1 in the solution decreases the emission intensity in the range of 525−640 nm significantly and increases the emission intensity of 650−700 nm remarkably. These findings indicate that FRET occurs. This finding corroborates the occurrence of the reaction from a certain number of pairs of ssDNAs to dsDNAs. A similar occurrence was also confirmed when the other concentration of 5′-Cy5-ST-1 was added to 5′-Cy3-ST-2.

Equation 3 was then used to perform the consistency analysis. The fraction of concentration can be found in Figure 1. The fluorophores, Cy3 and Cy5, have a Förster distance of 6 nm (where $\kappa^2 = 2/3$), which results in a value of 0.887 on the left side. The measurement result was 0.32 for the right side. This satisfies the inequality of eq 3. Therefore, it is certain that serious inconsistencies were avoided and FRET occurred.

Figure 3 shows the fluorescence intensity with respect to time. This shows the reaction kinetics in contrast to the emission scan, which can only show the intensity of the steady state. In Figure 3, the upper level of intensity in the steady state corresponds to the higher concentration of 5′-Cy5-ST-1.

Figure 4 shows the MEM fittings of these curves. Each row corresponds to a different concentration. From the top, this figure shows the result after an injection of 200 nM, 400 nM, 600 nM, 800 nM, and 1.0 μM of 5′-Cy5-ST-1. In the left panel (A1−A5), the smooth curves represent the fittings from MEM and the noisy curves are the actual data. From these fittings, the residues can be calculated (middle panel, B1−B5). It was confirmed that this is not the time-correlated noise using a power spectrum analysis (data not shown). The right panel (C1−C5) shows a $p(\log \tau)$ of eq 5.

From C1 to C5, a certain trend is shown. Here, the peak around $\log \tau \approx 1$ grows (except C4). This tendency appears to be valid because the higher concentration results in additional

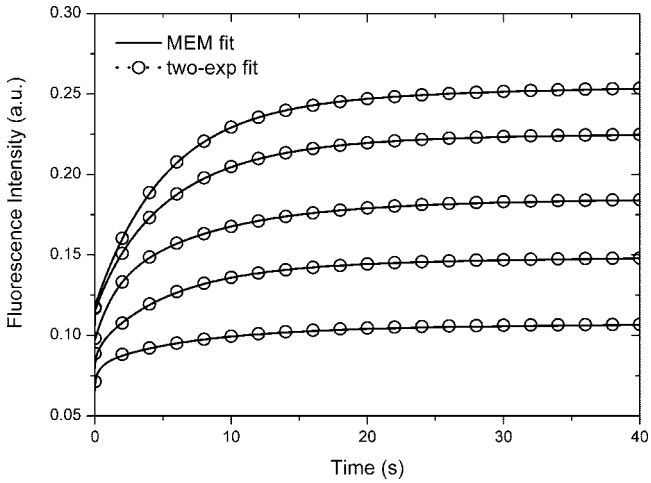

Figure 5. MEM fit (solid) and nonlinear fit to the two-exponential (dot and circle) function. The condition of each curve is similar to that in Figure 3.

reactions in solution. In C5, where the 5′-Cy5-ST-1 and 5′-Cy3-ST-2 have the same concentration, this peak moves sharply higher. Therefore, a careful conclusion would be that $\log \tau \approx 1$ is the relaxation time of the dominant reaction. Moreover, if the distribution p is sharp enough, p is employed as a multiplied local delta function. This results in the disappearance of the integral of eq 5. According to the features of bulk measurements, it can be expected that a high concentration provides more accuracy in the dominant kinetics. This expectation is simply assured by a simple inspection of the broadness of the peak (again, only C4 does not fit this theory).

The peaks of C1−C5 in Figure 4 mostly imply the existence of two significant types of kinetics, which is in agreement with the original assumption. To verify this assumption, the MEM fit was compared with the two-exponential fit. Figure 5 shows the nearly perfect overlaying of the MEM fit (solid line) over the two-exponential fit (dot and circle). Thus, consideration of only two dominant kinetics types is necessary to build a hypothesis.

In the solution, the setting of the chemical reaction is like the following.

$$5'\text{-Cy3-ST-2} + 5'\text{-Cy5-ST-1} \rightleftarrows \text{dsDNA}$$

Apparently, the chemical equilibrium of the above reaction provides most of the signal; hence, $\log \tau = 1$ (Figure 4) should be the relaxation time of the most dominant reaction.

NaCl is ionized in the solution, which makes the distance between the ssDNAs closer because of the neutralization of the native charge of DNA at its phosphate site. As a consequence of this, the energy to make the transition from ssDNAs to a dsDNA decreases. This transition appears to be single-step reaction, but the results indicate that, in a "certain condition", this reaction may have a transient intermediate state.

Figure 6 shows a diagram of the possible reaction. Mainly, a reaction from ssDNAs (on the left side) to the matched dsDNAs (on the right side) takes place. In addition, there may be other possibilities (middle panel) such as the formation of mismatched dsDNAs or ssDNAs that are close to each other.

In this experiment, the same volumes of 5′-Cy5-ST-1 were injected. After a sufficient mixing time, the concentration was homogeneous in all instances. On the other hand, it was not certain that the concentration was homogeneous directly after an injection. Immediately after an injection, a time trace measurement showed a decrease of the fluorescence intensity

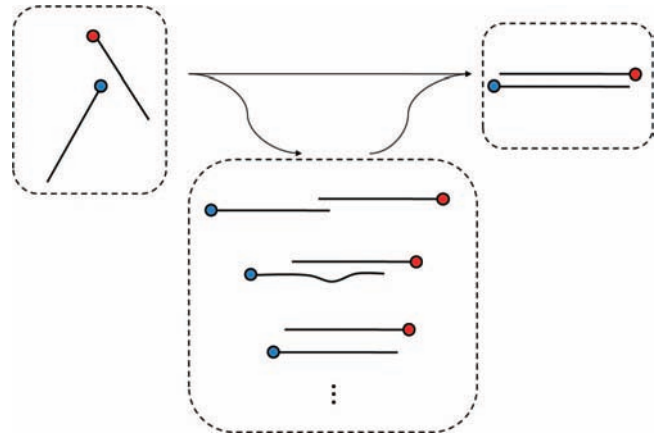

Figure 6. Representative diagram of the reaction in the experiments. The left side shows ssDNAs before the formation of dsDNA. The right side shows a matched dsDNA. The middle panel shows the various mismatched dsDNAs and ssDNAs that are close to each other.

for a short period. This piece of data was not included in the fitting for the sake of accuracy; hence, only raising part of the curve was fitted. After the 5′-Cy5-ST-1 solution was injected, the total volume expanded and the 5′-Cy3-ST-2 began to diffuse rapidly into a homogeneous state. Subsequently, 5′-Cy5-ST-1 immediately entered the beam incident region. These results imply that diffusion of ssDNAs is also homogeneously arranged as a reaction takes place. This represents the aforementioned "certain condition"; in this regime, the transient reaction in Figure 6 may be valid.

5. Conclusions

Equation 3 was used to verify the consistency of this experiment without a further experiment. This allowed us to confirm that the decrease of donor emission intensity is due to FRET phenomena, which results from the formation of dsDNA. Even if the UV absorbance measurements were performed, they should have been done under an environment that differed from that of the FRET measurement. Thus, it was necessary to verify the consistency of the FRET measurement separately. Equation 3 can be generalized if the extinction coefficient of the fluorophore, the acceptor emission, and the orientational factor are considered.

Measurements were also taken of the reaction kinetics of the complementary ssDNAs in the NaCl solution using the injection protocol. From the MEM fit and nonlinear curve fit, two major types of kinetics were detected. It is certain that one is the formation of matched dsDNA, and it was surmised that the other is the merged kinetics of all of the transient formations of mismatched DNA and ssDNAs that were close to each other.

The dynamics of DNA strands in a solution is important as this offers insight into an understanding of the mechanisms in which DNA is involved. Recent approaches to the reactions of DNA provide a microscopic view but typically require a complex optical setup and a diluted sample solution. In a cell, a denser environment is expected. The present study can be considered as a first step in an investigation of these dynamics in a dense solution involving a relatively simple optical scheme.

Acknowledgment. This work was supported by the Korea Science and Engineering Foundation (KOSEF) grant funded by the Korean government (MEST) (R0A-2007-000-20052-0).

References and Notes

(1) Schuler, B.; Lipman, E. A.; Eaton, W. A. *Nature* **2002**, *419*, 743–747.

(2) Dahan, M.; Deniz, A. A.; Ha, T.; Chemla, D. S.; Schultz, P. G.; Weiss, S. *Chem. Phys.* **1999**, *247*, 85–106.
(3) Hess, S. T.; Huang, S. H.; Heikal, A. A.; Webb, W. W. *Biochemistry* **2002**, *41*, 697–705.
(4) Haustein, E.; Schwille, P. *Methods* **2003**, *29*, 153–166.
(5) Förster, T. *Ann. Phys. (Berlin, Ger.)* **1948**, *437*, 55–75.
(6) van der Meer, B. W.; Coker, G., III; Chen, S.-Y. S. *Resonance Energy Transfer: Theory and Data*; VCH: New York, 1991.
(7) Lakowicz, J. R. *Principles of Fluorescence Spectroscopy*, 3rd ed.; Springer: New York, 2006.
(8) Rensselaer Polytechnic Institute. The DINAMelt Server. Prediction of Melting Profiles for Nucleic Acids. http://frontend.bioinfo.rpi.edu/applications/hybrid/hybrid2.php. Accessed: May 19, 2008.
(9) Dimitrov, R. A.; Zuker, M. *Biophys. J.* **2004**, *87*, 215–226.
(10) Epe, B.; Steinhäuser, K. G.; Woolley, P. *Proc. Natl. Acad. Sci. U.S.A.* **1983**, *80*, 2579–2583.
(11) Berney, C.; Danuser, G. *Biophys. J.* **2003**, *84*, 3992–4010.
(12) Dale, R. E.; Eisinger, J.; Blumberg, W. E. *Biophys. J.* **1979**, *26*, 161–193.
(13) Jares-Erijman, E. A.; Jovin, T. M. *J. Mol. Biol.* **1996**, *257*, 597–617.
(14) van der Meer, B. W. *Rev. Mol. Biotechnol.* **2002**, *82*, 181–196.
(15) VanBeek, D. B.; Zwier, M. C.; Shorb, J. M.; Krueger, B. P. *Biophys. J.* **2007**, *92*, 4168–4178.
(16) Skilling, J.; Bryan, R. K. *Mon. Not. R. Astron. Soc.* **1984**, *211*, 111–124.
(17) Sengupta, P.; Garai, K.; Balaji, J.; Periasamy, N.; Maiti, S. *Biophys. J.* **2003**, *84*, 1977–1984.
(18) Periasamy, N.; Verkman, A. S. *Biophys. J.* **1998**, *75*, 557–567.
(19) Steinbach, P. J.; Ionescu, R.; Matthews, C. R. *Biophys. J.* **2002**, *82*, 2244–2255.

JP8059695